

# TIME-FREQUENCY ANALYSIS OF A NOISY ULTRASOUND DOPPLER SIGNAL WITH A 2ND FIGURE EIGHT KERNEL

Yasuaki Noguchi<sup>1</sup>, Eiichi Kashiwagi<sup>2</sup>, Kohtaro Watanabe<sup>2</sup>, Fujihiko Matsumoto<sup>1</sup>  
and Suguru Sugimoto<sup>3</sup>

<sup>1</sup> Department of Applied Physics, National Defense Academy, Yokosuka, Japan

<sup>2</sup> Department of Computer Science, National Defense Academy, Yokosuka, Japan

<sup>3</sup> Faculty of Engineering, Shonnan Institute of Technology, Fujisawa, Japan

**Abstract**-Nonstationary ultrasound Doppler signals, those are changing with time and frequency simultaneously, are widely observed in biological and speech signals. A Cohen's class time-frequency (TF) analysis can analyze nonstationary signals with high resolution in time and frequency at a same time. A time-frequency distribution (TFD) is largely affected by a kernel function. Thus, there is sometimes a case where auto-terms (those are signal components) are covered by cross-terms (those are spurious components). In order to apply TFDs to a nonstationary and nonlinear Doppler ultrasound signals, experimental data were obtained by moving a steel ball to and fro by continuously irradiating it with ultrasound in olive oil. The movement of the steel ball was controlled by various functions. To analyze these signals, four kernels were used: (1) a Wigner kernel, (2) a Choi-Williams kernel, (3) a figure eight kernel, and (4) a 2nd figure eight kernel. Using our 2nd figure eight kernel, the demodulation accuracy was improved even with noise.

**Keywords**-Cohen's class, time-frequency analysis, Wigner distribution, Choi-Williams distribution, a figure eight kernel, a 2nd figure eight kernel, ultrasound Doppler signal

## 1 INTRODUCTION

A time-frequency (TF) analysis has been widely used recently for a biological signal analysis and a speech signal analysis in which dominant frequency components change with time. A Cohen's class TF analysis can analyze nonstationary signals with high accuracy [1].

A short-time Fourier transform (STFT) and its magnitude squared, a spectrogram, are known as the simplest and most useful TF transforms because they represent a generalization of traditional power spectral techniques to nonstationary signals. Although the STFT satisfies the properties, high-resolution spectra cannot be obtained due to the uncertainty relationship between time and frequency [2].

A Wigner distribution (WD) [3]- [5] has high resolution in time and frequency simultaneously in the TF plane. However, it does not satisfy the non-negative distribution condition. Moreover, the WD has many cross-terms, unavoidably generated by the bilinear structure of the Cohen's class TF distribution (TFD), which are spurious components. Thus, various kernel functions have been proposed to satisfy the required conditions of a kernel, such as the marginal condition, and to re-

duce the cross-terms [1], for example, RID [6, 7], Bessel distribution [8], and so on [9, 10].

In those kernels, a Choi-Williams distribution (CWD) [11] with an exponential kernel is a representative one. The CWD reduces cross-terms well for a chirp Doppler signal in which the Doppler shift changes linearly. Nevertheless, in a case where the Doppler shift changes sinusoidally, it is impossible to reduce the cross-terms even by the CWD.

Therefore, a new kernel, called a figure eight (FE) kernel, is proposed to reduce the cross-terms even in that case [12].

Furthermore, authors proposed a new kernel design method with new point of view [13]. The new kernel is called a 2nd figure eight (FE2) kernel.

There is no definite criteria what kernel should be utilized in the practical use. It depends on the characteristics of a signal to be analyzed. There is a proposal of a signal-dependent kernel function [14] that an ambiguity function is calculated first, and a kernel function adjusted to a shape of the ambiguity function is obtained.

However, in the case where the signal-to-noise ratio (S/N) is low, a signal-non-dependent kernel function should be designed to consider the characteristics of the signal. It is difficult to grasp the characteristics of the signal masked by the noise.

In this paper, for the first step to analyze the noisy biological nonstationary signal with high accuracy, TFDs are applied to simulation data, experimental data obtained by an ultrasound Doppler sinusoidal shift signal, and the noisy signal made from experimental data and synthesized noise.

The ultrasound Doppler sinusoidal shift signal is generated in olive oil by moving a steel ball to and fro by continuously irradiating it with ultrasound.

The TFDs are as follows: (1) WD, (2) CWD, (3) FE distribution (FED), and (4) FE2distribution (FE2D).

As a result, it is confirmed that a highly accurate TFD can be obtained with the FED even by a noisy signal, and a much more highly accurate TFD can be calculated with the FE2D.

## 2 COHEN'S CLASS TFD AND KERNEL FUNCTIONS

The Cohen's class TFD  $C(t, \omega)$  is defined as follows:

$$C(t, \omega) = \iiint e^{-j\theta t - j\tau\omega + j\theta u} \phi(\theta, \tau) z(u + \frac{\tau}{2}) \cdot z^*(u - \frac{\tau}{2}) du d\tau d\theta$$

## Report Documentation Page

<b>Report Date</b> 25 Oct 2001	<b>Report Type</b> N/A	<b>Dates Covered (from... to)</b> -
<b>Title and Subtitle</b> Time-Frequency Analysis of a Noisy Ultrasound Doppler Signal With a 2nd Figure Eight Kernel	<b>Contract Number</b>	
	<b>Grant Number</b>	
	<b>Program Element Number</b>	
<b>Author(s)</b>	<b>Project Number</b>	
	<b>Task Number</b>	
	<b>Work Unit Number</b>	
<b>Performing Organization Name(s) and Address(es)</b> Department of Applied Physics National Defense Academy Yokosuka, Japan	<b>Performing Organization Report Number</b>	
<b>Sponsoring/Monitoring Agency Name(s) and Address(es)</b> US Army Research, Development & Standardization Group (UK) PSC 802 Box 15 FPO AE 09499-1500	<b>Sponsor/Monitor's Acronym(s)</b>	
	<b>Sponsor/Monitor's Report Number(s)</b>	
<b>Distribution/Availability Statement</b> Approved for public release, distribution unlimited		
<b>Supplementary Notes</b> Papers from 23rd Annual International Conference of the IEEE Engineering in Medicine and Biology Society, October 25-28, 2001, held in Istanbul, Turkey. See also ADM001351 for entire conference on cd-rom.		
<b>Abstract</b>		
<b>Subject Terms</b>		
<b>Report Classification</b> unclassified	<b>Classification of this page</b> unclassified	
<b>Classification of Abstract</b> unclassified	<b>Limitation of Abstract</b> UU	
<b>Number of Pages</b> 4		

$$= \iint e^{-j\theta t - j\tau\omega} \phi(\theta, \tau) A(\theta, \tau) d\tau d\theta \quad (1)$$

$$A(\theta, \tau) = \int e^{j\theta u} z(u + \frac{\tau}{2}) z^*(u - \frac{\tau}{2}) du \quad (2)$$

where  $\phi(\theta, \tau)$  is a kernel function,  $z(t)$  is an analytic signal, and  $z^*(t)$  is a complex conjugate of  $z(t)$ . The term  $A(\theta, \tau)$  is an ambiguity function.

The TFD  $C(t, \omega)$  is directly influenced by the kernel  $\phi(\theta, \tau)$ . The kernel  $\phi(\theta, \tau)$  must satisfy requirements such that the TFD has the required properties [10].

In the case of  $\phi(\theta, \tau) = 1$ , the TFD is WD. To reduce the cross-terms of WD, various kernel functions have been proposed [1].

The CWD, which is an exponential function that has been proposed by Choi and Williams, reduces cross-terms and is good for linear chirp signal.

$$\phi(\theta, \tau) = e^{-\frac{\theta^2 \tau^2}{\sigma}} \quad (\sigma > 0) \quad (3)$$

CWD in this paper was calculated by  $\sigma = 2.0$ .

In order to ascertain a nature of an ambiguity function, the ambiguity function is calculated analytically [12] in the following two cases: (1) for a signal that is a sinusoidal and an ultrasound Doppler chirp (linear shift) signal, and (2) for a signal that is an ultrasound Doppler sinusoidal shift signal.

The analytic signal  $z(t)$  can be obtained from real data  $x(t)$  using two FFTs: a forward FFT of given real data, multiplication of the resulting positive harmonics by 2 and negative harmonics by 0, and then an inverse FFT.

The discrete expressions of Eqs. (1) and (2) are as follows:

$$A(p, m) = \sum_{i=0}^{N-1} z(i+m) z^*(i-m) W_N^{-pi} \quad (4)$$

$$C(n, k) = 2 \sum_{m=-\frac{N}{2}}^{\frac{N}{2}-1} \sum_{p=0}^{N-1} \phi(p, m) A(p, m) W_N^{pn} W_N^{mk} \quad (5)$$

where

$$W_N = e^{-j\frac{2\pi}{N}}. \quad (6)$$

In the case of a sinusoidal signal,  $A(\theta, \tau)$  is distributed only on the  $\tau$  axis in the  $(\theta, \tau)$  plane.

In the case of an ultrasound Doppler chirp (linear shift) signal,  $A(\theta, \tau)$  is on  $\theta = -c\tau$  in the  $(\theta, \tau)$  plane.

If we consider that one sinusoidal signal is shifted by one sinusoidal Doppler, the term  $A(\theta, \tau)$  is distributed like a figure eight around the  $\tau$  axis in the  $(\theta, \tau)$  plane.

### 3 A FIGURE EIGHT KERNEL [12]

From the previous considerations, it is clear that the ambiguity function has the following behavior. (1) The ambiguity function distributes on the  $\tau$  axis in the case of a sinusoidal signal, and (2) the ambiguity function distributes around the  $\tau$  axis in the case of an ultrasound Doppler sinusoidal shift signal.

On the other hand, it is already known that the auto-terms (original signals) distribute passing through the origin of the  $(\theta, \tau)$  plane, and the cross-terms (spurious signals) distribute passing through the other points separated from the origin.

$$\phi(\theta, \tau) = \begin{cases} \exp[-\frac{1}{\sigma}\{a^2\theta^2 - 4r^2(a^2 - \tau^2)\tau^2\}] & (\text{for } \{\cdot\} \geq 0) \\ 1 & (\text{for } \{\cdot\} < 0 \text{ and } \tau = 0) \end{cases} \quad (7)$$

$$r = \frac{b}{a}. \quad (8)$$

The discrete expression is as follows:

$$\phi(p, m) = \exp\left[-\left(\frac{2\pi}{N}\right)^2 \frac{1}{\sigma} \{a^2 p^2 - 4r^2(a^2 - m^2)m^2\}\right]. \quad (9)$$

Figure 1 shows a contour plot of the FE kernel. We call it a figure eight kernel as the shape of the contour plot looks like a figure 8.

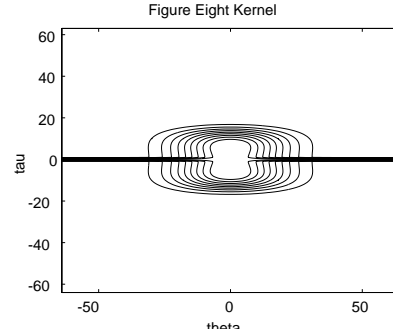


Figure 1: A contour plot of FE kernel.

In this paper, the FE kernel was calculated by  $N = 256$ ,  $a = N/16$ ,  $r = 1/2$ , and  $\sigma = N/4$ . When the TFD was calculated, each 128 data of both sides (total 256 data) were used. Thus, 512 data must be used to calculate if the TFD of 256 data was obtained.

### 4 A 2ND FIGURE EIGHT KERNEL [13]

The Cohen's class TFD  $C(t, \omega)$  is expressed as follows:

$$C(t, \omega) = \iint \int e^{-j\theta t - j\tau\omega + j\theta u} \phi(\theta, \tau) z(u + \frac{\tau}{2}) \cdot z^*(u - \frac{\tau}{2}) du d\tau d\theta \quad (10)$$

$$= \iint e^{-j\tau\omega} \Psi(\mu, \tau) z(t + \mu + \frac{\tau}{2}) \cdot z^*(t + \mu - \frac{\tau}{2}) d\mu d\tau \quad (11)$$

where  $\Psi(\mu, \tau)$  is an inverse Fourier transform of the kernel function  $\phi(\theta, \tau)$  with respect to  $\theta$ . The TFD  $C(t, \omega)$  is directly influenced by the kernel  $\phi(\theta, \tau)$  and an inverse of it,  $\Psi(\mu, \tau)$ .

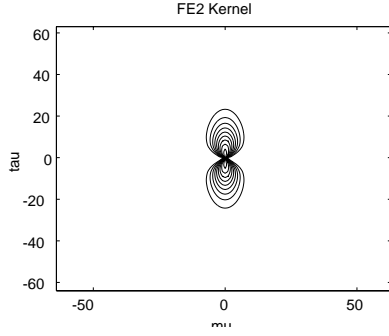


Figure 2: A contour plot of FE2 kernel.

Conventionally, the kernel was designed in the  $(\theta, \tau)$  plane.

However, in the case of a complicated signal, such as an ultrasound Doppler sinusoidal shift signal, the main part of the signal can be expected to distribute around the  $\tau$  axis like a fan [12].

In that case, it is more convenient to design the kernel in the  $(\mu, \tau)$  plane rather than in the  $(\theta, \tau)$  plane. When a quadratic or higher derivative of the signal frequency does not vanish, if  $\Psi(\mu, \tau)$  is taken wider for the  $\mu$  and  $\tau$  direction on the  $(\mu, \tau)$  plane, the frequency components shifted from the original frequency are added more and it becomes more difficult to calculate correct TF analysis [13].

Thus the authors proposed a new kernel design method. By the new method, the kernel satisfies the desired properties for a kernel [10]. Moreover, the kernel reduces the cross-terms and frequency shifts. That is

$$\Psi_{new}(\mu, \tau) = e^{-\frac{\tau^2}{\sigma^2}} \cdot e^{-\frac{\tau^2 + d^2}{d^2 + \tau^2} \mu^2} \sim \begin{cases} e^{-\frac{\tau^2}{\sigma^2}} \cdot e^{-\frac{\mu^2}{\tau^2}}, & |\tau| < d \\ e^{-\frac{\tau^2}{\sigma^2}} \cdot e^{-\frac{\mu^2}{d^2}}, & |\tau| > d \end{cases} \quad (12)$$

where,  $\Psi_{new}(0, 0)=1$ ,  $\Psi_{new}(\mu, 0) = 0(\mu \neq 0)$ .

Note that  $\Psi_{new}(\mu, \tau)$  is limited in the  $\mu$  direction by an exponential (reduces the cross-terms), and is also limited in the  $\tau$  direction (reduces the frequency shifts).

In Eq. (12), the contour lines with  $1/e$  in the  $\mu$  direction is  $\mu = \pm\tau$ , when  $|\tau| < d$ , and is  $\mu = \pm d$  when  $|\tau| > d$ . Thus the  $\Psi_{new}(\mu, \tau)$  can be designed to satisfy the time support property approximately and the shape of the distribution can be controlled by  $d$ .

Figure 2 shows a contour plot of the FE2 kernel. The FE2 in this paper was calculated by  $\sigma = N/8$  and  $d = N/20$ .

## 5 EXPERIMENT

A steel ball 8 mm in diameter was hung by a steel wire and submerged in olive oil in a container. The steel ball was set into motion by a sinusoid, triangular or square waves. An ultrasound transducer was placed on the extension of the orbit of the ball's movement. The transmission frequency was 1 MHz and the width of the trans-

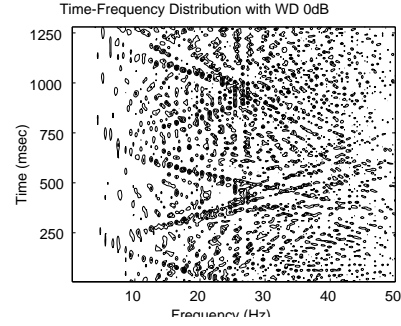


Figure 3: A contour plot of TFD with WD.

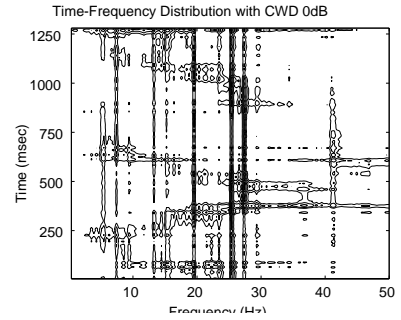
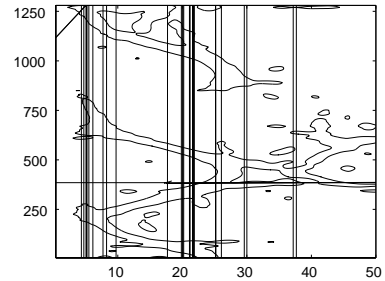


Figure 4: A contour plot of TFD with CWD.



mitted pulse was  $80 \mu\text{s}$ . The amplitude of the movement was regulated to obtain a sufficiently large Doppler signal. A band pass filter was used to remove the noise of the signal received after orthogonal detection with the transmitted signal. The sampling frequency was 200 Hz.

## 6 RESULTS AND DISCUSSION

The real biological data is somehow noisy. Hence, the experimental data are added by noise up to S/N 0 dB, that is, the noise is the same magnitude of the signal. Figures 3 – 6 show the TFDs obtained by the sinusoidal driving waveform with 0 dB noise and analyzed with WD, CWD, FED, and FE2D, respectively. These figures show contour plots of the positive part of TFD.

In spite that the distributions of spurious components spread over TF plane because of noise, the sinusoidal shift signal can be observed a little more clearly with WD shown in Fig. 3. From CWD shown in Fig. 4, it becomes also difficult to observe the sinusoidal shift signal clearly by adding the noise.

A portion of sinusoidal shift signal with FED shown in Fig. 5 is missing. On the other hand, the sinusoidal changes are rather well recognized by FE2D, shown in Fig. 6.

Our purpose is to get an exact analysis of a biological signal. Since the real biological signal can not avoid noise, the use of FE2 is advisable. Although the noise immunity of FED is low, we consider that FED can be useful to the S/N 6 dB because FED demodulates the sinusoidal components.

As a result, the new FE2 showed high resolution in TFD and the spurious components were reduced. The new FE2 can be used to analyze the TFD of the complicated ultrasound Doppler signal.

Using this new FE2, a real biological complicated signal, such as a signal from flowing blood, can be analyzed with TFD.

## 7 CONCLUSIONS

In this paper, we compare four TFDs of Cohen's class and investigate the applicability to the biological signals and speech signals. The simulation data and experimental data obtained by an ultrasound Doppler sinusoidal shift signal are utilized to obtain TFDs. Also the noisy signal is made from the experimental data and synthesized noise.

The ultrasound Doppler sinusoidal shift signal is generated in olive oil by moving a steel ball to and fro by continuously irradiating it with ultrasound.

The TFDs are (1) WD (Wigner distribution), (2) CWD (Choi-Williams distribution), (3) FED (figure eight distribution), and (4) FE2D (2nd figure eight distribution).

It is confirmed that a highly accurate TFD can be obtained with FED even by a noisy signal, and a much more highly accurate TFD can be calculated with FE2.

We can get a highly accurate TFD of a real complicated biological signal such as a blood flow signal or a heart sound signal. Furthermore, this result suggests the possibility that a characteristic of a signal, which

is overlooked by conventional spectral analyses, can be understood.

## References

- [1] L. Cohen, "Time-frequency analysis," Prentice Hall, Englewood Cliffs, NJ, 1995.
- [2] L. Cohen, "Time-Frequency Distributions - A Review," Proc. of the IEEE, vol.77, no.7, pp.941-981, July 1989.
- [3] T. A. C. M. Claasen and W. F. G. Mecklenbrauker, "The Wigner distribution - a tool for time-frequency signal analysis - Part 1: Continuous time signals," Philips J. of Research, vol.35, pp.217-250, 1980.
- [4] T. A. C. M. Claasen and W. F. G. Mecklenbrauker, "The Wigner distribution - A tool for time-frequency signal analysis - Part 2: Discrete time signals," Philips J. of Research, vol.35, pp.276-300, 1980.
- [5] T. A. C. M. Claasen and W. F. G. Mecklenbrauker, "The Wigner distribution - A tool for time-frequency signal analysis - Part 3: Relations with other time-frequency signal transformations," Philips J. of Research, vol.35, pp.372-389, 1980.
- [6] J. Jeong and W. Williams, "Kernel design for reduced interference distributions," IEEE Trans. on Signal Processing, vol.40, no.2, pp.402-412, Feb. 1992.
- [7] W. J. Williams, "Reduced interference distributions: Biological applications and interpretations," Proc. of the IEEE, vol.84, no.9, pp.1264-1280, Sep. 1996.
- [8] Z. Guo, L. Durand, and H. C. Lee, "The Time-Frequency Distributions of Nonstationary Signals Based on a Bessel Kernel," IEEE Trans. on Signal Processing, vol.42, no.7, pp.1700-1707, July 1994.
- [9] Y. Zhao, L. E. Atlas, and R. J. Marks, "The use of coneshaped kernels for generalized time-frequency representations of nonstationary signals," IEEE Trans. on Acoust. Speech & Signal Process., vol.38, no.7, pp.1084-1091, July 1990.
- [10] B. Boashash, "Time-frequency signal analysis," Longman Cheshire, Wiley Halsted Press, Australia, 1992.
- [11] H. Choi and W. J. Williams, "Improved time frequency representation of multicomponent signal using exponential kernels," IEEE Trans. on Acoust. Speech & Signal Process., vol.40, no.2, pp.402-412, Feb. 1992.
- [12] E. Kashiwagi, Y. Noguchi and K. Watanabe, "Proposal of Novel Eight-Figure Kernel for Time-Frequency Analysis," IEICE Trans., vol.J81-A, no.6, pp.907-915, June 1998.
- [13] K. Watanabe, Y. Noguchi and E. Kashiwagi, "A Method of Constructing the Kernel Function of Cohen's Class," IEICE Trans., vol.J81-A, no.12, pp.1802-1806, Dec. 1998.
- [14] B. Ristic and B. Boashash, "Kernel design for time-frequency signal analysis using the Radon transform," IEEE Trans. on Signal Processing, vol.41, no.5, pp.1996-2008, May 1993.